applied sciences

MDPI

Article

Tracing the Origins of an Anthropic Vitrified Structure with "Pre-Bleached with Blue LED" Thermoluminescence Dating: The Enigmatic Serravuda Hilltop Fortification in Calabria, Italy

Anna Galli [1], Miriam Saleh [1,*], Francesco Foggia [2] and Gian Paolo Sighinolfi [3]

[1] Department of Material Science, University of Milano-Bicocca, Via Cozzi 55, 20125 Milan, Italy; anna.galli@unimib.it
[2] Independent Researcher, 87041 Acri, Italy; foggia.francesco@libero.it
[3] Formerly Department of Chemical and Geological Sciences, University of Modena-Reggio Emilia, 41125 Modena, Italy; sighinolfig@yahoo.it
* Correspondence: m.saleh1@campus.unimib.it

Abstract: The Serravuda site on a hill near Acri, Calabria in Italy was discovered in 1970. The site presents a unique vitrified lithoid structure. Early theories speculated on its vitrification, ranging from forest fires to extraterrestrial impacts. The structure consists of vitrified Paleozoic rock fragments forming a 45-meter-long wall, possibly once extending further. Analysis suggests that humans transported these fragments for construction, with subsequent partial vitrification occurring due to high temperatures from wood combustion. Thermoluminescence dating, using the innovative "Pre-bleached with Blue LEDs" protocol, indicates origins between the Late Bronze Age and Iron Age, aligning with settlement periods in the region. Fading studies were conducted to correct the error in the age data due to signal loss. The scenario suggests that the vitrification of the structure may have been a consequence of human utilization of timber for construction, with combustion resulting from random events such as forest fires or lightning strikes. This description has remarkable similarities with to those proposed for Iron Age vitrified forts in Northern Europe, suggesting that Serravuda could be seen as a precursor to such forts. Moreover, this prompts intriguing inquiries into the origins and evolution of Nordic engineering techniques focused on fire utilization in construction.

Keywords: luminescence dating; thermoluminescence (TL); glass material; fortification; Mediterranean

Citation: Galli, A.; Saleh, M.; Foggia, F.; Sighinolfi, G.P. Tracing the Origins of an Anthropic Vitrified Structure with "Pre-Bleached with Blue LED" Thermoluminescence Dating: The Enigmatic Serravuda Hilltop Fortification in Calabria, Italy. *Appl. Sci.* **2024**, *14*, 4504. https://doi.org/10.3390/app14114504

Academic Editor: Richard Kouzes

Received: 2 May 2024
Revised: 14 May 2024
Accepted: 17 May 2024
Published: 24 May 2024

1. Introduction

During the Late Bronze Age and later Iron Age, it was common to discover fortifications strategically positioned on hilltops. However, fortifications that have been vitrified have so far only been found in continental and island northern Europe where they have been documented since the 1700s, and on which the current archaeological debate concerns the interpretation of their construction methods [1–3]. Comprehensive investigations of Scottish and, more recently, Swedish vitrified fortifications have been undertaken [4–8]. Interestingly, these architectural structures are predominantly found in insular Europe, although finds of vitrified structures have been reported over a broad strip developed in the E-W direction of continental Europe between Poland and Portugal. Apart from two cases encountered in the latter country [9,10], the presence of these structures has not yet been consistently observed in Mediterranean European countries.

The first announcement of the presence of molten rocks on the top of a hill called Serravuda at about 2 km North-West of Acri (Calabria, Italy, lat. 39°30′10.50″ N; long. 16°22′05.50″ E) was made by Francesco Foggia. This area is characterized by a series of

rounded peaks. What immediately captures one's attention is the presence of an intentionally levelled summit, surrounded by a mysterious glassy structure at its forefront that presents a distinctive elliptical shape. Bertolani [11], in the 1970s, authored a pioneering article on such vitrified rocks. In his analysis of the factors contributing to the vitrification process, the author examines a range of influences, including natural events like forest fires or lightning strikes, as well as human activities such as ceramic or metallurgical processes. Moreover, he explores the possibility of prehistoric or protohistoric rituals playing a role.

Recently, multidisciplinary research was conducted on Serravuda, covering lithology, mineralogy, and geochemistry. Part of these research results have already been published [12]. Mineralogical studies conducted confirmed that the vitrified materials had undergone pyrometamorphism at exceptionally high temperatures, ranging from 1000 to 1100 °C. Quantitative X-ray mineralogical and SEM analyses confirm that very high temperatures were reached as a result of the warming event, and in discussing the causes, they do not exclude the possible effects of an unusual lighting fulguration event [12].

A detailed geological mapping of the area and a series of lithological and petrographic investigations were conducted on the vitrified rock fragments found at the top of the hill, and on the exposed substrate rocks and other lithoid materials along the slopes of the hill [13]. These observations strongly suggest that the vitrified rock fragments are of allochthonous origin, indicating human intervention in their collection and transport for the construction of a hilltop structure.

Assuming an anthropogenic origin for such a structure, its absolute dating is of fundamental archaeological significance. It can provide information on potential builders and establish connections between them, and the human populations settled in the region at that time.

1.1. Serravuda's Rocks Geology and Morphology

Geologically, the area where outcrops of fused rocks were found is part of the Sila Plateau [11]. It is therefore constituted by crystalline basement rocks originated from igneous plutons intruding during the Carboniferous and Permian subduction which were uplifted and metamorphosed by the creation of the Apennines and erosion [14]. The basement consists of a variety of medium-high grade metamorphic terrains that include kinzigitic (biotite-sillimanite and garnet-bearing) gneiss, amphibolites, and granitoid bodies (migmatites).

The metamorphites in the area have often undergone significant retro-metamorphism, changing to greenschist facies [15]. The landscape, characterized by outcrops of vitrified rocks, features a series of hills and rounded reliefs oriented mainly in a north-south direction. Among these, Serravuda stands out with its summit 926 m above sea level. Its distinguishing feature is the almost elliptical flattened summit that measures 32 m in a W-E direction and 25 m in a N-S direction [11].

A recent comprehensive geological survey of the Serravuda region, helped by the complete disappearance of vegetation following a fire in July 2023, revealed intriguing discoveries [13]. At the top of the hill, where vitrified rock fragments are present, only granitic substrate rocks emerge. However, along the slopes at lower elevations, the substrate is dominated by metamorphites, mainly gneiss. The scattered lithoid fragments, embedded in the alteration mantle that covers the slopes, reflect the substrate rocks in their petrographic composition. These erratics, which represent more than 90 percent of the volume, present elongated and angular features, different from the rounded pebbles typically associated with the disintegration of granitoid rocks.

Generalities on the Structure of Vitrified Rocks

Bertolani [11] initially presented data on the spatial distribution and petrographic characteristics of the vitrified rocks on Serravuda Hill. Recently, other authors added further insights [11,13]. The vitrification process involved the upper portion of a rocky debris

deposit localized along the northern and northwestern edges of the flat hilltop. This deposit forms an elongated structure, arched at the ends, like a wall about 45 m long (20 m and 25 m each part) and with an average thickness of about one meter (see Figure 1).

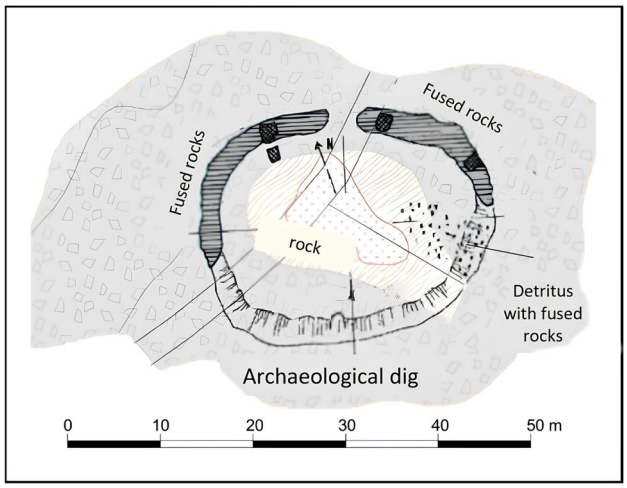

Figure 1. Simplified geological map of the top of Mt. Serravuda.

Excavations conducted by Bertolani in the 1970s and recent excavations for the installation of telecommunication antennas have allowed for an understanding of the stratigraphy of the detrital deposit. The vitrification process covered the upper portion of the wall structure along its entire length, forming a continuous and compact vitrified crust of varying thickness, which in some areas exceeds 80–90 cm.

Below the compact vitrified crust, between 30 and 60 cm deep, is a layer of reddish oxidized rock fragments overlying other detrital materials with a black surface. At a depth of 1.40–1.50 m, the base of the deposit consists of material fragmented directly on granitoid rocks similar to those on the surface of the hill. Since the outcrops of vitrified rock stuck out of the ground by several tens of centimeters in the 1970s, it can be assumed that the original height of the deposit of rock debris exceeded two meters.

A comprehensive examination of the shape, size, and litho-petrographic traits of the construction materials reveals a striking consistency: they primarily consist of fragments of metamorphites. These materials, making up over 90% of the volume, closely resemble the loose erratics found within the alteration mantle covering the relief slopes [16]. Observations of the spatial arrangement of the rock fragments present in the vitrified structure indicate that they were constructed by vertically stacking larger rock fragments on top of each other and placing smaller rock fragments in the gaps [13].

These findings indicate once more, beyond reasonable doubt, the anthropic origin for the Serravuda structure and man not only as an agent of material collection and transportation but also as an engineer.

Field observations conducted since July 2023 led to the discovery of significant volumes of vitrified rock fragments along the SE and SW slopes of Serravuda Hill, most of which were concentrated near the flattened summit [13]. The location of these materials suggests that they were originally allocated to the edges of the flattened summit surfaces and from there slid down the slopes due to landslides. Recent studies suggest that they originally constituted a wall structure like the one still present on the N and NE sides of the hill, which had suffered complete destruction. In this case, the original construction may have had a more or less closed circular or sub-circular shape (Figure 1), similar to common ancient, fortified structures.

Surface excavations conducted in the 1970s on the southern side of the Serravuda hilltop, on the other hand, yielded fragments of pottery characterized by distinct types attributable to the 4th–2nd century B.C., proving that ancient Italic populations (maybe the Brutii) inhabited and settled in the region at that time.

1.2. Dating Vitrified Structures

The initial attempts at dating the forts directly involved the utilization of the radiocarbon method [17–19]. However, uncertainties and doubts afflicted these early efforts, such as calibrating the radiocarbon timeline and determining the amount of radiocarbon present in such ancient times. An attempt to date with archaeomagnetism has been trued on the vitrified wall at the Misericordia, Serpa, Portugal, Late Bronze Age site [10].

Thermoluminescence, developed for personal and environmental dosimetry [20], and proposed for determining the age of ancient ceramics [21,22], was subsequently applied to date various other types of heated archaeological materials, such as burnt flint and stones (see, for example, [23]). It was applied by Sanderson at the end of the eighties to the vitrified forts [6,24]. From his more recent paper [5], it appears that this dating technique is promising even if the application seems to be related to a particular firing temperature. In more recent years, studies focused on the luminescence properties and the TL dating feasibility of archaeological glass [25] have highlighted that the mosaic tesserae are particularly suitable for dosimetric analysis by means of TL. This paper delves into an intriguing archaeological–geological case that demands an absolute chronology for partial resolution. To address this, the implementation of an experimental protocol based on thermoluminescence dosimetry, the "Pre-bleached with Blue LED" protocol, is suggested. This method, originally developed for studying accidental dosimeters in mobile phone displays [26], has shown success when applied to Islamic mosaic tesserae [27].

Discher and Woda's (2013) protocol has a significant advantage in its ability to overcome the limitations of classical thermoluminescence methodology only. This is achieved by isolating a thermally more stable TL signal and establishing a fading curve. Although this methodology adequately addresses incidental dosimetry, its direct applicability to archaeological dating is limited. The distinction lies in the nature of the dosimetric events: incidental dosimetry involves instantaneous and intense ionizing events, with doses significantly higher than those from natural and clearly defined sources over time. Dating, on the other hand, involves an extended period of time. By simultaneously examining fading, information on signal loss and trap characteristics can be obtained, aiding reinterpretation.

2. Materials and Methods

2.1. Samples

The samples considered in the present study were collected during a series of investigation campaigns during which outcropping substrate rocks were collected both on the top of Serravuda Hill and along the slopes of the hill itself, as well as fragmented material accumulated on the top of the hill itself and showing evidence of having undergone pyrometamorphism and vitrification.

Previously published work by Elmi et al. (2021) provided detailed descriptions and general data, including location, quantitative X-ray mineral analysis, and petrographic attributions of the individual samples collected [12].

Among these samples, fourteen rock fragment samples from the vitrified structure, which showed evidence of prometamorphism, were selected for thermoluminescence (TL) dating. Such evidence consists of reddening, macro- and micro-fracturing, and, above all, the presence of a vitreous component testifying the material underwent partial melting with consequent formation of liquids able to percolate throughout rock fragments.

In addition, a sample of substrate rock (named sample SE 9) was collected from the Serravuda hill. This sample was not affected by the heating event that caused the vitrification, thus serving as a crucial confirmation for the method employed.

The selection of samples for analysis was initially guided by their mineralogy, with a preference for granitoid samples rich in quartz and feldspars and poor in Fe-rich phases. These samples were considered more suitable for conventional TL methodologies, as

confirmed by previous research [21]. Based on their mineralogy, glass phase content, and location, they can be classified into distinct groups (see Table 1).

Table 1. Samples and typology analyzed.

Typology	Sample Code
Granitoid substrate rock unaffected by heating	SE9
Heated or partially melted granitoid rocks fragments (6 samples)	SE2, SE6, SE13, SV1 3P, SV 4C, SV6
Heated or partially melted metamorphic rocks fragments (3 samples)	SE7, SE12, SV5
Vitreous cements (4 samples)	SV 1A, SV 1B, SV 1 3V, SV 4V

Although granitoid pyrometamorphites are a relatively minor component (<5% volume) within the vitrified structure, they typically occur as small, rounded pebbles of about 10 cm. They exhibit pronounced macro- and micro-deformation, with only slight indications of partial melting.

The metamorphic pyrometamorphite fragments (85% volume) consist of kinzigitic gneisses or their retro-metamorphic counterparts. Morphologically distinct from granitoids, these fragments exhibit elongated shapes and sharp edges, often accompanied by an amorphous component. These characteristics imply significant involvement in the partial melting process during the heating event.

The term "vitreous cements" includes all pyrometamorphic products in which optical microscopy reveals a predominant amorphous component. A portion of amorphous liquid has managed to flow between the un-melted rock fragments, effectively binding them together. These cements appear as thin glassy crusts enclosing the rock fragments (e.g., samples SV 1–4 and SV4-V), as veins of dense material without bubbles (SV 1-A), or as accumulations within pockets containing dense black glass (sample SV 1–3V) or considerably vesicular pumice glass (SV1-B).

For the preparation of thermoluminescence measurements of samples, an extensive granulometric grinding process was carried out using a stainless-steel mortar to prepare the sample to the measurement. This entire procedure was executed in the dim red laboratory light. The selection of particle size was necessary, considering the instrument's irradiation and measurement requirements, and it included grain sizes within the intervals of <125 μm, 125–250 μm, and 250–500 μm. Macroscopically ground samples exhibit varying colors and aspects, with many of them appearing very dark.

2.2. Thermoluminescence Methodology

All measurements were conducted using a Risø TL/OSL DA-20 system (Centre for Nuclear Technologies, Technical University of Denmark, DTU Risø Campus, Roskilde, Denmark), equipped with a 90Sr-90Y beta source, delivering an irradiation dose rate of 0.11 Gy s^{-1} (±3%).

Thermoluminescence (TL) measurements were recorded at a rate of 2 °C/s, employing a bi-alkali photomultiplier tube (EMI 9235QB, ET-Enterprises Ltd., Uxbridge, UK) and a 7.5-mm Hoya U-340 filter (Edmund Optics, Barrington, NJ, USA), selectively transmitting in the 280–380 nm region, with maximum transmittance (57%) at 330 nm. The excitation source for illumination used a blue LED array (470 ± 30 nm) with a constant stimulating power of 54 mW cm^{-2}. The "a" value determination has been evaluated by using a 37 MBq ^{241}Am calibrated external alpha source, providing a dose rate of 14.8 Gy min^{-1}.

Dose Rate Evaluation

The values of ^{40}K, ^{238}U, and ^{232}Th were obtained through ICP-MS analysis. Powdered samples were digested with concentrated HF and HNO_3, (both of suprapuR grade), dried down, and re-dissolved. Before analysis, samples were diluted with MilliQ water to a final HNO_3 concentration of 4% *w*/*w*. Measures were made of the Centro InTErdipartimentale Grandi Strumenti (UNIMORE) using a quadrupole ICP-MS (Thermo Fisher Scientific, Waltham, MA, USA, Xseries9) using classical methods (data on the contents of radioisotopes K, U, and Th in all analyzed samples were gently furnished by Anna Cipriani and Federico Lugli (Department of Chemical and Geological Sciences, University of Modena and Reggio E., Italy)).

To calculate the contribution of soil to the dose rate, average ppm values of radionuclides for each category were considered. Therefore, the average value of the concentrations of ^{238}U, ^{232}Th, and ^{40}K was considered. The external gamma contribution was primarily based on the radioactivity within a 30-centimeter-diameter sphere centered at the sampling point, estimated for each sample by considering its radioactivity and that of its surroundings [21,28]. An additional 0.16 mGy a^{-1} contribution from cosmic rays was included. Refer to Table 2 for specific values.

Table 2. Dose rate measurements' results.

Sample	Water Content (%)	^{238}U (ppm; ±5%)	^{232}Th (ppm; ±5%)	^{40}K (ppm; ±3%)	Internal Dose Rate (mGy a^{-1}; ±5%)	External Dose Rate (mGy a^{-1}; ±5%)
SE9	7	0.37	20.75	1.21	1.52	0.62
SE2	7	0.06	1.08	1.22	0.83	0.68
SE6	7	0.09	1.03	1.22	0.83	0.62
SE7	7	0.15	0.42	1.22	0.82	0.68
SE12	7	0.26	1.29	1.22	0.87	0.68
SE13	7	0.43	17.32	1.22	1.47	0.68
SV 13P	7	0.19	4.67	1.22	0.82	0.68
SV 4C	7	0.04	0.21	1.22	0.79	0.68
SV5	7	0.14	1.95	1.22	0.87	0.68
SV6	7	0.22	0.39	1.22	0.83	0.68
SV 1A	7	0.37	5.91	2.01	1.53	0.65
SV 1B	7	1.59	12.02	2.01	1.93	0.65
SV 13V	7	0.47	7.94	2.01	1.60	0.68
SV 4V	7	0.27	1.01	2.01	1.34	0.68

2.3. Measurement Protocol

The "Pre-Bleached with Blue LED" Protocol involves exposing the vitreous sample to blue LED light for a duration of 500 s, followed by evaluation of the accident dose and calibration dose signals. A significant adjustment was made to the incident dosimetry protocol for the sieved rocks extracted from the wall, where the incident dose was compared to the equivalent dose.

The measurement procedure involved three dose irradiations of 5.5, 11 and 16.5 Gy, respectively. Signal integration was conducted within the 85–140 channel, corresponding to a temperature range of 150 °C to 250 °C. In addition, thermoluminescence measurements were performed up to 450 °C at a heating rate of 2 °C/s (Table 3).

In order to evaluate the effectiveness of the applied blue LED, a "classical" thermoluminescence protocol was introduced for comparative analysis. This additional step ensures a comprehensive evaluation of the results obtained with "Pre-bleached with Blue LED" approach, providing a broader understanding of the thermoluminescent properties of glassy samples (Table 4). It is therefore to be considered as a qualitative and not a quantitative evaluation with a comparison of the obtained dates.

Table 3. Pre-bleached with blue LED protocol, where a, b, c correspond to the 3 different doses given during treatment in the 3 different cycles.

Step	Treatment	
1	500 s blue LED bleaching	Natural TL
2	TL 450 °C, 2 °C/s	
3	[a] 5.5 Gy (50 s β) [b] 11 Gy (100 s β) [c] 16.5 Gy (150 s β)	TL Growth
4	500 s blue LED bleaching	
5	TL 450 °C, 2 °C/s	

Table 4. Classical thermoluminescence (TL) protocol.

Step	Treatment	
1	TL 450 °C, 2 °C/s	Natural TL
2	[a] 5.5 Gy (50 s β) [b] 11 Gy (100 s β) [c] 16.5 Gy (150 s β)	TL Growth
3	TL 450 °C, 2 °C/s	

2.4. Anomalous Fading Correction

Anomalous fading represents an inadvertent occurrence affecting thermoluminescence (TL). This phenomenon manifests in certain minerals, where luminescence intensity is contingent on the elapsed time since irradiation. The term "anomalous" is employed due to its propensity to unexpectedly release trapped electrons. Notably, electrons that should remain trapped at room temperature are liberated earlier than anticipated, often within a few days, rendering them unsuitable for precise dating.

The significance of anomalous fading in TL dating was initially emphasized by Wintle in 1973, leading to the integration of anomalous fading tests into measurement protocols [29]. Subsequently, Aitken proposed a model based on tunneling mechanisms to elucidate this phenomenon in 1985 [21]. Aitken's model introduced a logarithmic law to delineate the signal decay: $ln\ (T/Tc)$.

This relationship characterizes the luminescence intensity versus time:

$$I = I_C\left(1 - k\ ln\left(\frac{T}{T_C}\right)\right) \quad (1)$$

Considering the intensity I_c at an arbitrary time (T_C), and κ is a constant, characteristic of the sample. In archaeological materials, continuous exposure to natural radiation, maintaining a proportional relationship with age, must be considered. Nevertheless, through the integration of Equation (1), it becomes possible to determine that T represents the true age, contrasting with T_F, which denotes the fading age.

$$\frac{T_F}{T} = 1 - k\ \left[\ln\left(\frac{T}{T_C}\right) - 1\right] \quad (2)$$

The origin of the tunnelling model lies in the data derived from feldspar fading studies [30]. However, its applicability to different materials remains uncertain. On the other hand, the absence of a universal model can be addressed through the delineation of empirical data. Discher and Woda propose an ingenious solution by exploring the attenuation resulting from a single ionizing event [26]. Their research has evolved to include incident dosimetry for phone displays. They model the empirical behavior of TL intensity over time, fitting it perfectly to the outlines of a hyperbolic curve plotted directly on experimental data. Here A, B, and C are specific parameters of the sample.

$$I = \frac{A}{(1 + BT)^C} \quad (3)$$

The study extends Dischер and Woda's model to amorphous materials, as evident in the analysis of mosaic tiles, adhering to the superposition principle illustrated by Huntley and Lamothe. The trend of fading should be examined for all samples over a fixed period of time and considering several aliquots. By integrating the normalized dose over time and replacing parameters A, B, and C, the corrected age for fading is determined:

$$\frac{T_{fad}}{T} = \frac{1}{T}\int_0^T \frac{I(T - t')}{I_0}\, dt' = \frac{1}{T}\frac{A}{B\,(1 - C)}[(1 + BT)^{1-C} - 1] \quad (4)$$

It is worth noting that since age, adsorbed dose and thermoluminescence intensity are all proportionally related, there is no distinction in describing abnormal fading in terms of T_{Fad}/T, I_{Fad}/I or D_{Fad}/D, as pointed out by Huntley and Lamothe in 2001 [30].

3. Results

In all samples, the curves showed continuous growth consistent in their patterns (Figure 2), while the thermoluminescence curves showed different trends based on the characteristics of each sample, outlining distinct patterns for each typology (Figure 3).

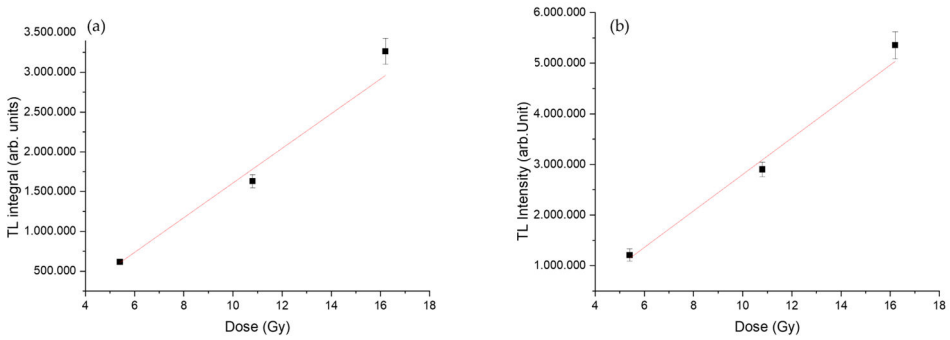

Figure 2. TL signal growth as a function of applied beta dose (5.5, 11, 16.5 Gy) in (**a**) sample SE2 and (**b**) sample SE13. The signal refers to the results of the "Pre-bleached with Blue LED" protocol.

Examination of the thermoluminescence (TL) curves revealed five distinctive trends, two of which are specifically associated with heated or partially vitrified rocks. It is remarkable that these trends show no correlation with the presence or absence of heating indicators or other intrinsic rock characteristics.

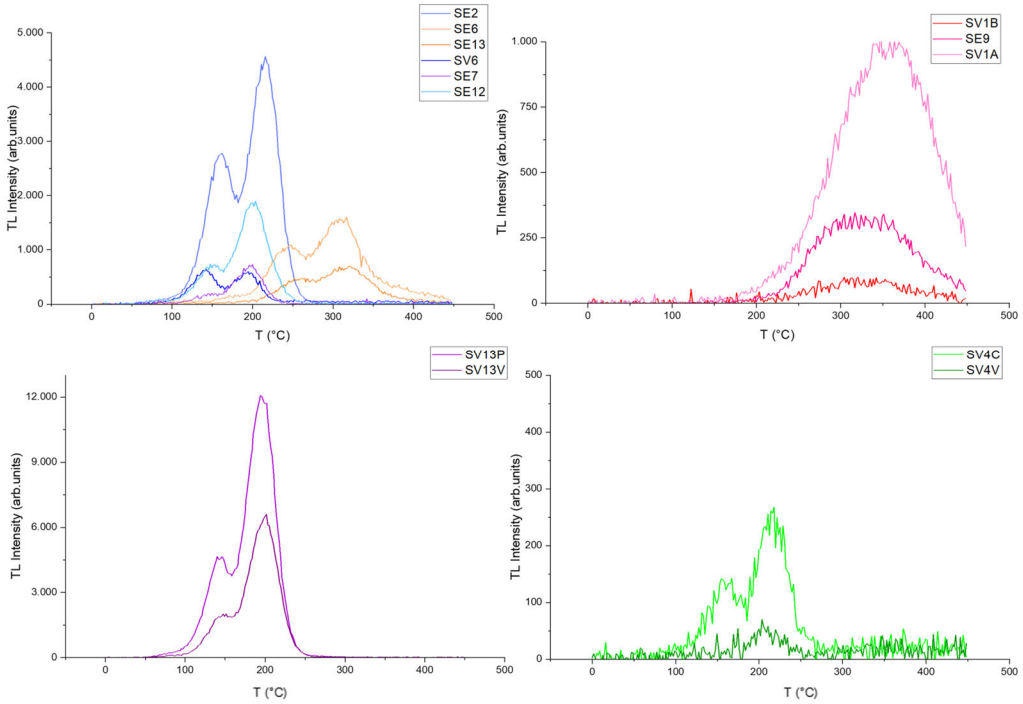

Figure 3. Comparison of natural TL curves for each typology. The signals refer to the results of the "Pre-bleach with Blue LED" protocol.

In contrast, when examining the natural thermoluminescence (TL) curves of samples from identical blocks, such as SV4V and SV4C, or SV13V and SV13P, no noteworthy distinctions are observed, despite the different initial typology. However, in the case of SE9 and its two associated samples, SV1A and SV1B, a significant increase in the natural TL incandescence curve becomes evident after crossing the 200 °C threshold.

Furthermore, as introduced before, the curves of the samples were evaluated using a classical thermoluminescence measurement, without further steps. A comparison of some of the curves of samples using the "Pre-bleached with Blue LED" method and a classical thermoluminescence protocol is shown in Figure 4 to emphasize how the method proposed in this work cuts out all of the signal before 100 °C.

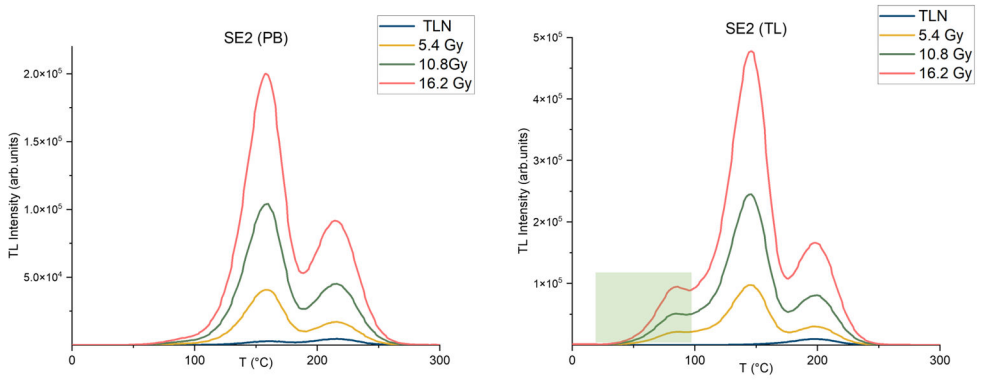

Figure 4. Comparison of signal growth curves of samples SE2 with the "Pre-bleached with Blue LED" protocol (**left**) and the classical one (**right**). In the green part, the corresponding signal loss can be observed.

Samples showing fading were corrected using the integration method described in Section 2.4 above. It is crucial to emphasize that fading is not uniformly present in all aliquots. Fading was observed in specific aliquots of four samples: SE2, SE13, SV13P, and SV5, except for sample SV5, where all aliquots showed fading. To perform the correction

process, an ad hoc solution was created by scripting a code in Matlab [The Math Works, Inc., Natick, MA, USA, MATLAB, version 2020a.].

An in-depth analysis of signal loss was carried out, lasting at least one month, and involving at least two aliquots of each sample. Figure 5 shows one of the fading trends for reference.

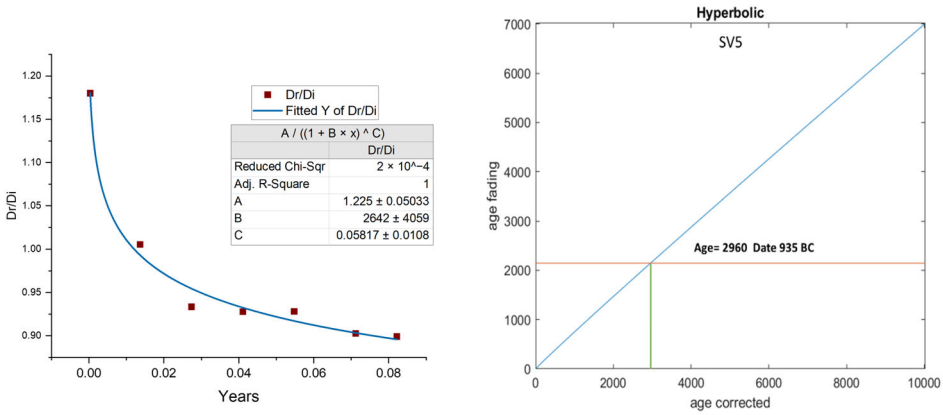

Figure 5. Example of the fading curve following one month of analysis (**left**). Experimental data have been normalized relative to the imparted dose of 8.25 Gy. The initial data point is derived immediately after the first minute, followed by subsequent measure. (**Right**) In the figure on the right the results of the hyperbolic fading correction curve with the correct age value reading on the x-axis.

Upon completion of the equivalent dose assessment utilizing the 'pre-bleached with blue LED' protocol and subsequent dose rate calculations, the age of the samples was determined (see Table 5). The uncertainties associated with these age calculations were computed following the principles of error propagation, as illustrated in Figure 6 and Table 6.

Table 5. Equivalent dose and dose rate values.

Sample	Equivalent Dose (ED) (Gy)	Dose Rate (mGy y^{-1})
SE9	150.0 ± 39.0	2.09 ± 0.05
SE2	3.28 ± 0.36	1.41 ± 0.05
SE6	136.0 ± 19.0	1.40 ± 0.05
SE7	2.73 ± 0.06	1.40 ± 0.05
SE12	3.60 ± 0.08	1.44 ± 0.05
SE13	2.93 ± 0.18	2.04 ± 0.05
SV 13P	3.99 ± 0.55	1.40 ± 0.05
SV 4C	4.10 ± 0.28	1.37 ± 0.05
SV5	3.10 ± 0.42	1.44 ± 0.05
SV6	4.26 ± 0.02	1.41 ± 0.05
SV 1A	3.43 ± 1.52	2.12 ± 0.05
SV 1B	4.16 ± 0.34	2.52 ± 0.05
SV 13V	3.50 ± 0.26	2.18 ± 0.05
SV 4V	3.68 ± 0.03	1.43 ± 0.05

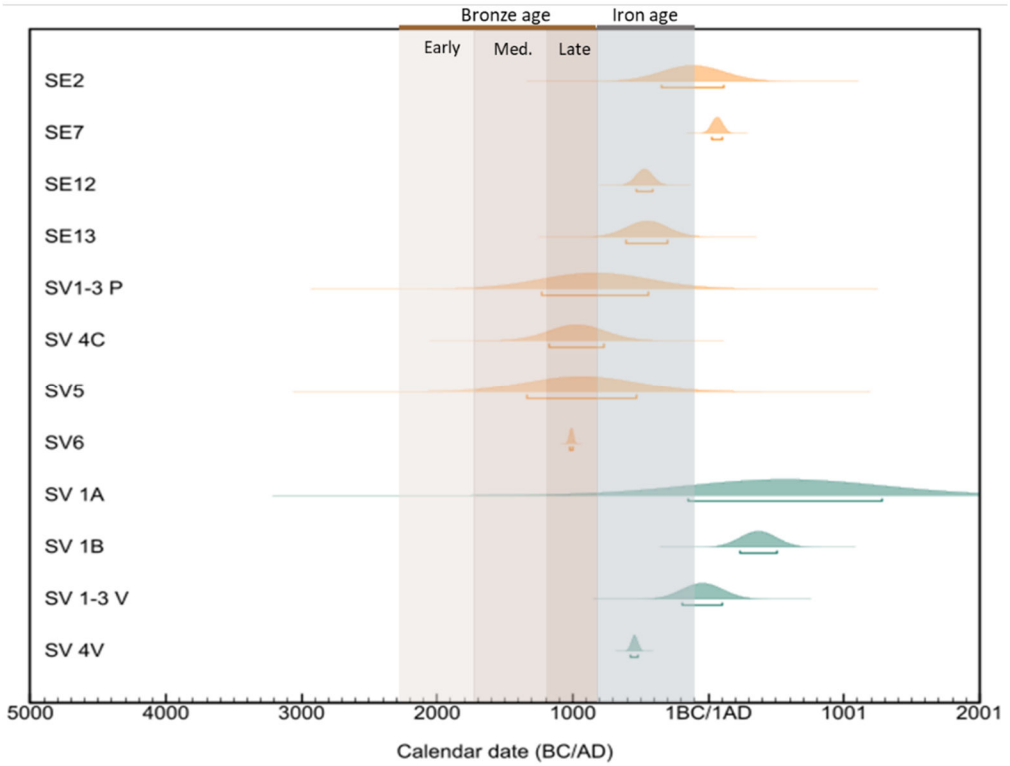

Figure 6. Final date ranges in correspondence to the Bronze and Iron Ages in southern Italy. In orange are samples belonging to the category of heated or partially vitrified rocks. In light blue are the vitreous cements.

Table 6. Age estimation for each sample typology.

Sample Code	Proposed Age
Heated or partially melted granitoid rocks	
SE2	115 BCE ± 230
SE13	450 BCE ± 150
SV1 3P	835 BCE ± 395
SV 4C	970 BCE ± 205
SV6	1010 BCE ± 15
Heated or partially melted metamorphic rocks	
SE7	67 CE ± 40
SE12	470 BCE ± 60
SV5	935 BCE ± 400
Vitreous cements	
SV 1A	566 CE ± 710
SV 1B	370 CE ± 130
SV1 3V	42 BCE ± 150
SV 4V	543 BCE ± 20

4. Discussion

4.1. Age Results Discussion

The available data on the equivalent dose conclusively affirm that SE9, a granitoid substrate rock unaffected by pyrometamorphism, has retained its original characteristics over time, placing it firmly within a distinct geological era. Used as a benchmark, SE9 sample provided a means to evaluate the effectiveness of the method.

Remarkably, sample SE6 also behaves like sample SE9. It therefore appears to have retained its geological age. SE6 corresponds to a granitoid rock fragment collected at the top of the vitrified structure and showing macroscopic indications of pyrometamorphism. This fact is difficult to explain. According to the analyses of Elmi et. al., its mineralogy is rather peculiar [12]. Noteworthy is the uncommon presence of traces of the high-pressure cohesite phase together with cristobalite, combined with the absence of other heating indicators. A possible explanation for this inconsistency is that the mineralogy of this rock fragment located at the surface of the vitrified structure was influenced not only by the heating event due to wood combustion, but also by a shock metamorphic event correlated to lighting strikes. For clarity of the image range, the results of SE9 and SE6 are not shown graphically in Figure 6.

The TL dating of all analyzed samples shows a wide range of age values (1740 BCE to 550 CE). The glass cements, consisting mainly of amorphous components (glass), are significantly younger than rock fragments that have undergone only a small partial melting.

Theoretically, the large dispersion of calculated ages could be related to distinct episodes of heating and vitrification that occurred over time. However, a solid set of evidence seems to dismiss this possibility. It has been seen that the pyrometamorphism that affected the upper portion of the structure led to the formation of a single (up to 90 cm) and compact vitrified crust. Within this crust, there are no facies variations traditionally associated with weathering or indicative of discontinuous and repetitive heating events, so that it appears justified to assume that the vitrification of the structure was achieved as a result of a single episode that occurred within a given time interval.

The significant age differences measured in the glass cements characterized by very low crystallinity compared to the pyrometamorphite samples affected by relatively low partial melting suggest that these age discrepancies can be attributed to intrinsic limitations of the measurement protocol.

These limitations appear to be closely related to the dosimetric properties of quartz in the glassy matrix, a topic extensively discussed in the 2019 paper by Galli et al. [27].

A parallel investigation is underway to assess the potential impact of self-absorption in the light signal, possibly influenced by the dark color of the vitreous cements, which were found to be younger than the granitoid pyrometamorphites (Table 6).

In this context, it is worth noting that the iron (Fe) content in vitreous cement samples, especially those of recent origin, can be remarkably high (up to 26.24% Fe_2O_3, as reported by A. Cipriani (University of Modena and Reggio Emilia), personal communication, in sharp contrast to the Fe content observed in rock fragment samples with granitoid composition.

In the framework of a unique pyrometamorphic event responsible the vitrification of the structure, the current focus is on determining the most likely age of this conversion.

Therefore, excluding the data on vitreous cement and the data on the anomalous age of the SE 7 sample (Table 6), it is reasonable to conclude that the vitrification of the Serravuda structure took place between 1010 and 470 BCe, i.e., during the Late Bronze Age and Early Iron Age.

4.2. The Purpose behind the Serravuda Hilltop Structure

After proposing the anthropogenic origin of the vitrified structure of Serravuda and confirming the thermoluminescence data, the discussion shifts from its age, plausibly dating to the Late Bronze and Early Iron Age, to its destination and events that contributed to its vitrification. These two aspects may be connected. As early as 1972, Bertolani speculated that the Serravuda vitrified rocks in the area could be the remains of pottery smelting furnaces or closed furnaces for the production of metals or alloys [11]. Consequently, the vitrification of the materials could be linked to human use of the structure. The possibility that ceramic activities took place on the summit of Serravuda in ancient times was initially considered due to the discovery, previously cited, of ceramic remains dating back to the

4th–2nd centuries BCE [11]. Nevertheless, several considerations, such as the location of the structures on the summit of a relief and their shape and size, as well as the absence of argillaceous material in the area, make this hypothesis completely implausible.

Moreover, the size and geometry of the construction erected on the summit of Serravuda and our on-site observation on geochemical data relating to "technophilic" metals such as Cu, Zn, Ni, Co, Ag suggest a metallurgical furnace was built on the site highly improbable

Excluding therefore the possibility that the vitrification of the Serravuda structure is linked to specific human activities involving fire, one can only assume this structure was erected exclusively for defensive purposes.

There are a series of evidence to support this thesis. Firstly, the structure is built on the edges of an artificially flattened summit of the highest regional relief. Furthermore, its narrow, elongated shape is reminiscent of a defensive wall. Some evidence suggests that it originally extended along the entire perimeter of the hill [13]. Therefore, both its substantial dimensions and the construction techniques used align with the defensive structures known as "wall circuits", widespread in southern Italy [31]. These structures were built as early as the Early Bronze Age and saw significant expansion during the Iron Age, often associated with specific episodes of colonization of the region. Of particular interest in this context are the settlements of populations in areas very close to Serravuda, as documented in the of Colle Dogna site in Acri [32,33]. In addition, the presence in Calabria of successive populations, namely the Oenotrians, Brutii, and then Romans, who settled in the region more or less permanently, in the time interval between the Middle Bronze and Early Iron Ages, is widely documented in the literature [34–37].

Based on these considerations, it can be affirmed that the fortified construction of Serravuda fits in well with the knowledge of the presence of human settlements in Calabria and Southern Italy in general. The fact remains that it is distinguished from all others solely by the fact that it underwent vitrification. This fact prompts a comparative discussion regarding vitrification processes that occurred in Serravuda and other ancient fortifications, particularly Iron Age vitrified forts in Northern Europe.

4.3. Vitrification Techniques in Ancient Anthropic Structure and Proposed Scenario at Serravuda

Having stressed once again that vitrification of lithoid materials can also occur as a consequence of natural processes or as a result of specific human activities including the use of fire, only vitrification processes that affected ancient constructions erected for defensive purposes, i.e., fortified structures, will be discussed here. In this regard, it must be emphasized that in archaeological history, the term 'vitrification' denotes a construction technique in which man uses fire to raise temperatures to the point of partially melting lithoid materials. The aim is to generate liquids that, when cooled, undergo partial recrystallisation or turn into glass, thus binding the melted components together and strengthening the structure [38,39]. As reported before, one of the best known examples of vitrification processes is provided by the so-called 'vitrified forts' that represent a hallmark of the Iron age civilization in northern continental and island Europe [4,8,9,40].

Here, as occurred at the Serravuda site, the heat source capable of reaching the temperatures required for vitrification consist in the combustion of woody materials (timbers, logs, poles, and branches). Wooden materials were incorporated within loose rock fragments which normally were used to construct defensive structures.

In dealing with the vitrification processes characterizing the vitrified forts of northern Europe, there have been some aspects that have been much discussed over the years, some of which are still somewhat controversial. One of these concerns is precisely about the presence and purpose of the inclusion of woody material in a structure fundamentally composed of fragmented lithoid material. After many studies and discussions on the typology of such materials, it is now generally agreed that in the case of the Nordic vitrified forts, timber was introduced by man not to facilitate the erection of a vertically developed structure, but solely to act as fuel in order to obtain a source of heat sufficient to melt the

rocks, aiding their vitrification. The silicate liquids produced during melting, flowing through the loose lithoid materials, had the tendency to bond them, acting as cement.

Concerning this hypothesized process, scientists of the northern forts have long wondered whether the combustion of wood, the only source of heat available in those ancient times, was sufficient to induce significant vitrification of the lithoid material used for construction. This is because the mineral paragenesis observed in pyrometamorphosed materials and, in particular, the quench crystalline phases present in the glass matrix, suggest that frequently, very high temperatures (of the order of 1000–1100 °C) were attained during the heating event [4,17,41–43].

At this point, it should be noted that the SEM (scanning electron microscope) and X-ray diffraction (XRD) data of Elmi et al. [12] on the Serravuda rocks also provided similar thermometric indications. Similarities were also observed in the high-temperature mineral phase assemblages and in the quench, products present in the vitreous matrix. What distinguishes Serravuda from most North European vitrified forts is the overabundance of vitreous matter acting as a cement, as evidenced by the formation of a homogeneous vitreous crust of high thickness (up to 90 cm). This indicates that large volumes of liquid were generated during a single heating event, and this evidence does not support the hypothesis that only sporadic temperature peaks were reached. A possible interpretation of the overabundance of liquids at Serravuda is provided by the observations and results of some geochemical studies carried out on some vitrified forts in Scotland [7,44]. Here, the partial melting process involved lithoid materials very similar to those at Serravuda (predominantly metamorphic crystalline rocks particularly rich in biotite and other hydrated silicate phases) and led to the formation of extensive volumes of vitrified liquids. According to the hypothesis of these authors, when biotite-rich materials are involved in partial melting, liquid formation can occur at relatively modest temperatures (800–850 °C) as a result of processes that deviate from granitic melting models, which include a series of reactions mainly involving biotite and other hydrated phyllosilicates as key reactants.

That a similar pattern acted at Serravuda is suggested by both the large volumes of liquids produced and their composition. Indeed, when liquids are formed at very low temperatures, one would expect the presence of huge volumes of vitrified materials. Furthermore, the mafic character of Serravuda glasses, characterized by a high iron content, explains their cementing effects related to their property of flowing between un-melted rock fragments due to their low viscosity.

Although considerations of partial melting patterns have highlighted certain similarities in shrinkage between Serravuda and, at least, some northern European vitrified forts, there are certain aspects related to the origin of the heating event and the presence and purpose of the woody material added to the lithoid component that tend, in addition to significant differences in age, to discriminate the Serravuda structure from northern forts.

Based on current interpretations, it seems well established that timber was introduced by man with the sole purpose of intentionally igniting the vitrification process of the lithoid material to strengthen the defensive structure. In the case of Serravuda, we would exclude this interpretation, believing this hypothesis to be technologically too advanced and beyond the capabilities of man at that time. Now, on this topic, as on the causes of the heating event, we can only make assumptions, the most plausible of which are given in the following scenario that aims to illustrate what might have happened at Serravuda.

Italic populations settled in the mountainous terrain of inner Calabria and the Sila massif as early as the Middle Bronze Age, if not earlier. They built defensive structures on top of Serravuda hill, the most elevated peak in the region. The only available building material consisted of fragments of crystalline rocks (essentially metamorphites) found among the altered mantle covering the slopes of the hill and transported by man to the summit. The relatively small size (decametric) of rock fragments created difficulties in erecting vertical defensive structures. To overcome this obstacle, builders incorporated in the structure considerable amounts of woody materials for the sole purpose of erecting

the structure vertically and thereby stabilizing it. As a result of natural events and processes such as forest fires or lightning strikes or, alternatively, because of daily human activities, the woody component of the structure would have undergone a combustion process resulting in the partial destruction and partial vitrification of the Serravuda structure.

We are perfectly conscious that this scenario is only hypothetical for the moment, but in the current state of knowledge, it is the most probable. At the same time, it raises even more questions as to how and when Northern European engineers learned the sophisticated construction technique of vitrified forts based on the use of fire.

5. Conclusions

This research on Serravuda vitrified rocks initially was conducted to clarify whether human activity or natural events were the driving forces behind their construction. It is an exemplary demonstration of how a multidisciplinary approach can generate hypotheses to solve these ancient mysteries. Observations on the lithological nature and mineralogical and petrographic studies on utilized materials suggest the role of man in constructing a probably old defensive structure. To confirm this hypothesis, the "Pre-bleached with Blue LED" TL protocol, originally designed for different purposes, has proven yielding promising results in determining the age of the Serravuda fortified structure.

To strengthen these initial hypotheses and support the thesis of ancient activities, thermoluminescence analysis proved to be a valid method of analysis. The dating of glass materials presents intrinsic challenges due to their structural properties; however, the "Pre-bleached with Blue LED" protocol has proven adaptable.

Many of these samples can be reliably dated to at least 3000 years ago, strongly indicating their origin during a period when signs of settlement in the analyzed area were evident.

The obtained data on the Serravuda vitrified rocks not only provided crucial clues to the dating of heating events, but also underline the feasibility of the used TL protocol as a potential tool for dating any kind of glass material, avoiding the challenges often encountered with traditional thermoluminescence. Moreover, it is worth underlining that these results made it possible to cross-reference the obtained data and to reconstruct the relative chronology by defining the occupation period of the settlement of the area.

Another noteworthy comment is the remarkable similarity between the construction and vitrification of Serravuda and the vitrified forts found in northern Europe. This similarity extends to several aspects, including the common purpose of defensive fortification, the use of crystalline siliceous rocks as construction materials, and the common cause of vitrification: a heating episode triggered by the burning of timber incorporated during construction.

However, dating suggests that Serravuda was probably built by human hands more than a millennium before the construction of defensive structures in northern Europe, where intentional vitrification was used for structural reinforcement. Unlike the deliberate vitrification techniques employed by Northern Iron Age peoples, the vitrification of Serravuda probably occurred inadvertently, as a result of an accidental event. This crucial distinction emphasizes that Serravuda vitrification was not a deliberate construction method similar to those universally adopted in northern European regions.

Despite the contrasting origins of the vitrification process and its deliberate use by humans, the significant similarities outlined previously between the Middle Bronze to Early Iron Age structure of Serravuda and Iron Age defensive constructions in northern Europe led us to classify Serravuda as a vitrified proto-fortress. This classification underlines its importance as a unique discovery, as Serravuda represents the only example so far identified not only in southern Italy, but in the entire southern Mediterranean region.

At this point, the possibility of the existence of proto-vitrified forts similar to Serravuda also raises intriguing questions about the origin of the vitrified forts of northern

Europe. Questions emerge about how and when Northern Iron Age engineers learned the technique of vitrification to build their forts. It is not unreasonable to think that somewhere in northern Europe and at an unspecified time, an event like the one that occurred in Serravuda took place. The accidental destruction by fire of a fortified structure made of fragments of rock and timber and its subsequent vitrification would have become a commonly applied construction technique. Accepting this scenario plausibly, proto-vitrified forts must also have existed in continental and insular northern Europe.

Author Contributions: Conceptualization, A.G.; Data curation, M.S.; Formal analysis, A.G., M.S. and G.P.S.; Investigation, A.G., M.S., F.F. and G.P.S.; Methodology, A.G.; Resources, A.G., F.F. and G.P.S.; Software, M.S.; Supervision, A.G.; Validation, A.G. and M.S.; Visualization, M.S.; Writing—original draft, A.G., M.S. and G.P.S. All authors have read and agreed to the published version of the manuscript.

Funding: This research received no external funding.

Data Availability Statement: The original contributions presented in the study are included in the article, further inquiries can be directed to the corresponding author.

Acknowledgments: The authors would like to thank Anna Cipriani and Federico Lugli, department of Chemistry and Geological Sciences, University of Modena and Reggio Emilia and the Archeologist Massimo Di Salvatore for its useful advice and contribution in carrying out this research.

Conflicts of Interest: The authors declare no conflict of interest.

References

1. M'Hardy, C.B. On Vitrified Forts, with Results of Experiments as to the Probable Manner in Which Their Vitrification May Have Been Produced. *Proc. Soc.* **1906**, *40*, 136–150.
2. Childe, V.G. Excavation of the Vitrified Fort of Finavon, Angus. *Proc. Soc. Antiqu. Scotl.* **1935**, *69*, 49–80. https://doi.org/10.9750/PSAS.069.49.80.
3. Childe, V.G.; Thorneycroft, W.; Desch, C.H. The Vitrified Fort at Rahoy, Morvern, Argyll. *Proc. Soc. Antiqu. Scotl.* **1938**, *72*, 23–43. https://doi.org/10.9750/PSAS.072.23.43.
4. McCloy, J.S.; Marcial, J.; Clarke, J.S.; Ahmadzadeh, M.; Wolff, J.A.; Vicenzi, E.P.; Bollinger, D.L.; Ogenhall, E.; Englund, M.; Pearce, C.I.; et al. Reproduction of Melting Behavior for Vitrified Hillforts Based on Amphibolite, Granite, and Basalt Lithologies. *Sci. Rep.* **2021**, *11*, 1272. https://doi.org/10.1038/s41598-020-80485-w.
5. Sanderson, D.C.W.; Placido, F.; Tate, J.O. Scottish Vitrified Forts: TL Results from Six Study Sites. *Int. J. Radiat. Appl. Instrumentation. Part D Nucl. Tracks Radiat. Meas.* **1988**, *14*, 307–316. https://doi.org/10.1016/1359-0189(88)90081-7.
6. Sanderson, D.C.W.; Placido, F.; Tate, J.O. Scottish Vitrified Forts: Background and Potential for TL Dating. *Nucl. Tracks Radiat. Meas.* **1985**, *10*, 799–809. https://doi.org/10.1016/0735-245X(85)90093-6.
7. Friend, C.R.L.; Kirby, J.E.; Charnley, N.R.; Dye, J. New Field, Analytical Data and Melting Temperature Determinations from Three Vitrified Forts in Lochaber, Western Highlands, Scotland. *J. Archaeol. Sci. Rep.* **2016**, *10*, 237–252. https://doi.org/10.1016/j.jasrep.2016.09.015.
8. Kresten, P.; Ambrosiani, B. Swedish Vitrified Forts—A Reconnaissance Study. *J. Swed. Antiqu. Res.* **1992**, 1–17.
9. Berrocal-Rangel, L.; García-Giménez, R.; Ruano, L.; Vigil de la Villa, R. Vitrified Walls in the Iron Age of Western Iberia: New Research from an Archaeometric Perspective. *Eur. J. Archaeol.* **2019**, *22*, 185–209. https://doi.org/10.1017/eaa.2018.69.
10. Catanzariti, G.; McIntosh, G.; Monge Soares, A.M.; Díaz-Martínez, E.; Kresten, P.; Osete, M.L. Archaeomagnetic Dating of a Vitrified Wall at the Late Bronze Age Settlement of Misericordia (Serpa, Portugal). *J. Archaeol. Sci.* **2008**, *35*, 1399–1407. https://doi.org/10.1016/j.jas.2007.10.004.
11. Bertolani, M. An Enigmatic Outcrop of Vitrified Rocks near Acri (Cosenza). *Boll. Della Soc. Geol. Ital.* **1972**, *91*, 683–692.
12. Elmi, C.; Cipriani, A.; Lugli, F.; Sighinolfi, G. Insights on the Origin of Vitrified Rocks from Serravuda, Acri (Italy): Rock Fulgurite or Anthropogenic Activity? *Geosciences* **2021**, *11*, 493. https://doi.org/10.3390/geosciences11120493.
13. Foggia, F.; Sighinolfi, G.P.; Tosatti, G. Lithological Features and Provenance of the Material Used for the Construction of the Serravuda Hilltop Vitrified Structure (Calabria, Italy). *Atti. Soc. Nat. Mat. di Modena* **2024**, 1–12, *in press*.
14. Doglioni, C.; Flores, G. *Encyclopedia of European and Asian Regional Geology*; Moores, E.M., Fairbridge, R.W., Eds.; Springer: Dordrecht, The Netherlands, 1997; pp. 414–435.
15. Bertolani, M.; Foggia, F. La Formazione Kinzigitica Della Sila Greca. *Boll. Soc. Geol. It.* **1975**, *91*, 683–692.
16. Borrelli, L.; Critelli, S.; Gulla, G.; Muto, F. *Rilievo Del Grado Di Alterazione Delle Rocce Cristalline*; presentazione della carta del grado di alterazione e dei movimenti di massa della porzione Centro-Occidentale del Bacino Del F. Mucone; Geologi Calabria: Catanzaro, Italy, 2011; pp. 3–46.
17. Nisbet, H.C. A Geological Approach to Vitrified Forts. *Sci. Archaeol* **1974**, *12*, 3–12.
18. Greig, C. Excavations at Castle Point, Troup, Banffshire. *Aberdeen Uni. Rev* **1970**, *43*, 274–283.

19. Mackie, E.W. *The Vitrified Forts of Scotland*; Academic Press: Cambridge, MA, USA, 1976.
20. Daniels, F.; Boyd, C.A.; Saunders, D.F. Thermoluminescence as a Research Tool. *Science* **1953**, *117*, 343–349. https://doi.org/10.1126/science.117.3040.343.
21. Aitken, M.J. *Thermoluminescence Dating*; Academic Press: London, UK, 1985.
22. Galli, A.; Sibilia, E.; Martini, M. Ceramic Chronology by Luminescence Dating: How and When It Is Possible to Date Ceramic Artefacts. *Archaeol. Anthropol. Sci.* **2020**, *12*, 190. https://doi.org/10.1007/s12520-020-01140-z.
23. Wagner, G.A. *Age Determination of Young Rocks and Artifacts Physical and Chemical Clocks in Quaternary Geology and Archaeology*; Natural Science in Archaeology; Springer: Berlin/Heidelberg, Germany, 1988.
24. Sanderson, D.C.W.; Warren, S.E.; Hunter, J.R. *The TL Properties of Archaeological Glass*; Risoe National Laboratory: Roskilde, Denmark, 1983; ISBN 87-550-0915-8.
25. Galli, A.; Poldi, G.; Martini, M.; Sibilia, E.; Montanari, C.; Panzeri, L. Study of Blue Colour in Ancient Mosaic Tesserae by Means of Thermoluminescence and Reflectance Measurements. *Appl. Phys. A* **2006**, *83*, 675–679. https://doi.org/10.1007/s00339-006-3588-y.
26. Discher, M.; Woda, C. Thermoluminescence of Glass Display from Mobile Phones for Retrospective and Accident Dosimetry. *Radiat. Meas.* **2013**, *53–54*, 12–21. https://doi.org/10.1016/j.radmeas.2013.04.002.
27. Galli, A.; Caccia, M.; Martini, M.; Panzeri, L.; Maspero, F.; Fiorentino, S.; Vandini, M.; Sibilia, E. Applying the "Pre-Bleached with Blue LEDs" Protocol to Date Umayyad Mosaic Tesserae by Thermoluminescence. *Quat. Geochronol.* **2019**, *49*, 218–222. https://doi.org/10.1016/j.quageo.2018.05.014.
28. Guérin, G.; Mercier, N.; Adamiec, G. Dose-Rate Conversion Factors: Update. *Anc. TL* **2011**, *29*, 5.
29. Wintle, A.G. Anomalous Fading of Thermo-Luminescence in Mineral Samples. *Nature* **1973**, *245*, 143–144. https://doi.org/10.1038/245143a0.
30. Huntley, D.J.; Lamothe, M. Ubiquity of Anomalous Fading in K-Feldspars and the Measurement and Correction for It in Optical Dating. *Can. J. Earth Sci.* **2001**, *38*, 1093–1106. https://doi.org/10.1139/e01-013.
31. Gualtieri, M. Fortifications and Settlement Organization: An Example from pre-Roman Italy. *World Archaeol.* **1987**, *19*, 30–46. https://doi.org/10.1080/00438243.1987.9980022.
32. Castagna, M.A.; Ferranti, F.; Levi, S.T.; Luppino, S.; Peroni, R.; Schiappelli, A.; Vanzetti, A. Broglio Di Trebisacce, Cittavetere Di Saracena, Colle Dogna Di Acri, Campagna 1999. In Proceedings of the Convegno Magna Grecia e Oriente mediterraneo prima dell'età ellenistica, Taranto, Italy, 1–5 October 1999.
33. Castagna, M.A.; Schiappelli, A. La Sequenza Stratigrafica Di Acri-Colle Dogna (CS), Tra Eneolitico e Bronzo Antico. In Proceedings of the Atti della XXXVII Riunione Scientifica dell'Istituto Italiano diPreistoria e Protostoria, Tortora, Italy, 29 September–4 October 2002.
34. Jung, R.; Mommsen, H.; Pacciarelli, M. From West to West: Determining Production Regions of Mycenaean Pottery of Punta Di Zambrone (Calabria, Italy). *J. Archaeol. Sci. Rep.* **2015**, *3*, 455–463. https://doi.org/10.1016/j.jasrep.2015.07.004.
35. Marino, D.; Pacciarelli, M. Calabria. L'antica Età Del Bronzo. Articolazioni Culturali e Cronologiche. In Proceedings of the Atti del Congresso Nazionale "L'antica età del bronzo in Italia", Viareggio, Italy, 9–12 January 1995; pp. 147–162.
36. Taliano Grasso, A.; Marino, D.; Nicoletti, G.; Medaglia, S. Rocche Protostoriche e Abitati Brettii Tra Sila e Mare Jonio. In Proceedings of the Atti convegno internazionale Centri fortificati indigeni della Calabria dalla protostoria all'età ellenistica, Napoli, Italy, 16–17 January 2014.
37. Sevink, J.; De Neef, W.; Vito, M.A.D.; Arienzo, I.; Attema, P.A.; Van Loon, E.E.; Ullrich, B.; Den Haan, M.; Ippolito, F.; Noorda, N. A Multidisciplinary Study of an Exceptional Prehistoric Waste Dump in the Mountainous Inland of Calabria (Italy): Implications for Reconstructions of Prehistoric Land Use and Vegetation in Southern Italy. *Holocene* **2020**, *30*, 1310–1331. https://doi.org/10.1177/0959683620919974.
38. Mackie, E.W. Timber-Laced and Vitrified Walls in Iron Age Forts: Causes of Vitrification. *Glasg. Archaeol. J.* **1969**, *1*, 69–71. https://doi.org/10.3366/gas.1969.1.1.69.
39. D.R. Brothwell, A.C. Bishop, A.R. Woolley Vitrified Forts in Scotland: A Problem in Interpretation and Primitive Technology. *J. Archaeol. Sci.* **1974**, *1*, 101–107.
40. Kresten, P.; Goedicke, C.; Manzano, A. TL-Dating of Vitrified Material. *Geochronometria* **2003**, *22*, 9–14.
41. Youngblood, E.; Fredriksson, B.J.; Kraut, F.; Fredriksson, K. Celtic Vitrified Forts: Implications of a Chemical-Petrological Study of Glasses and Source Rocks. *J. Archaeol. Sci.* **1978**, *5*, 99–121.
42. Smith, D.C.; Vernioles, J.D. The Temperature of Fusion of a Celtic Vitrified Fort: A Feasibility Study of the Application of the Raman Microprobe to the Non-Destructive Characterization of Unprepared Archaeological Objects. *J. Raman Spectrosc.* **1998**, *28*, 195–198.

43. Wadsworth, F.B.; Heap, M.J.; Damby, D.E.; Hess, K.-U.; Najorka, J.; Vasseur, J.; Fahrner, D.; Dingwell, D.B. Local Geology Controlled the Feasibility of Vitrifying Iron Age Buildings. *Sci. Rep.* **2017**, *7*, 40028. https://doi.org/10.1038/srep40028.
44. Friend, C.R.L.; Dye, J.; Fowler, M.B. New Field and Geochemical Evidence from Vitrified Forts in South Morar and Moidart, NW Scotland: Further Insight into Melting and the Process of Vitrification. *J. Archaeol. Sci.* **2007**, *34*, 1685–1701. https://doi.org/10.1016/j.jas.2006.12.007.